

Document downloaded from:

<http://hdl.handle.net/10251/166592>

This paper must be cited as:

Salavert, F.; Navarro Bohigues, JA.; Owen, CA.; Khechmar, S.; Pallás Benet, V.; Livieratos, IC. (2020). Cucurbit chlorotic yellows virus p22 suppressor of RNA silencing binds single-, double-stranded long and short interfering RNA molecules in vitro. *Virus Research*. 279:1-8. <https://doi.org/10.1016/j.virusres.2020.197887>



The final publication is available at

<https://doi.org/10.1016/j.virusres.2020.197887>

Copyright Elsevier

Additional Information

1
2
3 ***Cucurbit chlorotic yellows virus p22 suppressor of RNA silencing binds single-, double-stranded long and short***
4 ***interfering RNA molecules in vitro***
5
6

7 Ferran Salavert^a, José Antonio Navarro^b, Carolyn A. Owen^a, Souheyla Khechmar^a, Vicente Pallás^b and Ioannis C.
8 Livieratos^{a,*}
9

10
11
12 ^a *Department of Sustainable Agriculture, Mediterranean Agronomic Institute of Chania, Alysio Agrokepion, GR-73100,*
13 *Chania, Crete, Greece*

14 ^b *Instituto de Biología Molecular y Celular de Plantas, Universidad Politecnica de Valencia-CSIC, Av. de los Naranjos*
15 *s/n, 46022, Valencia, Spain*
16
17
18
19

20
21
22 **ABSTRACT**
23
24

25 *Cucurbit chlorotic yellows virus* (CCYV) p22 has recently been reported to be a weak local suppressor of RNA silencing
26 for which interaction with cucumber SKP1LB1 through an F-box-like motif was demonstrated to be essential. Using a
27 bacterially expressed maltose-binding protein (MBP) fusion of CCYV p22 in electrophoretic mobility shift assays (EMSA),
28 we have examined *in vitro* its ability to bind different RNA templates. Our experiments showed that CCYV p22 is able to
29 bind to ss and ds long RNAs, in addition to ss and ds siRNA molecules. CCYV p22 deletion mutants (MBP_CCYV DEL1-
30 4) were produced that covered the entire protein, with MBP_CCYV DEL2 corresponding to the F-box motif and its
31 flanking sequences. None of these deletions abolished the capacity of CCYV p22 to bind ss- and dsRNA molecules.
32 However, deletions affecting the C-ter middle part of the protein did not efficiently bind either ss- or dsRNA molecules
33 indicating that essential elements for this interaction are located in this region. Our EMSA experiments showed an
34 increased affinity for CCYV p22 binding 24 nt-long ss siRNAs, which agrees with the previous report of reduced
35 accumulation of siRNAs in GFP/ CCYV p22 agroinfiltrated leaf patches. Taken together, our data adds to current
36 knowledge of the mode of action of suppressors of RNA silencing encoded by genes sited at the 3'-terminus of crinivirus
37 genomic RNA 1, and shed light on the involvement of CCYV p22 in the suppression of RNA silencing or/and in another
38 role in the virus life cycle *via* RNA binding.
39
40
41
42
43
44
45
46

47 **Keywords:** criniviruses, RNA binding, *Cucurbit chlorotic yellows virus*, whitefly-transmitted viruses, suppressor of RNA
48 silencing
49

50
51 * Corresponding author: +30 28210 35050; Fax: +30 28210 35001.

52 *E-mail address:* livieratos@maich.gr (I. C. Livieratos)
53
54
55
56
57
58
59

1. Introduction

Cucurbit chlorotic yellows virus (CCYV) is a newly-assigned member of the genus *Crinivirus* (Gyoutoku et al., 2009), first observed in greenhouse-grown melons in Japan (2004). CCYV infections have been reported in cucurbit crops in Asia, North Africa, the Mediterranean basin and, recently, in the United States (Huang et al., 2010; Abrahamian et al., 2013; Bananej et al., 2013; Orfanidou et al., 2014; Wintermantel et al., 2019). The symptomatology of CCYV (leaf yellowing) and natural transmission by *Bemisia tabaci* whitefly biotypes MEAM1 and MED does not differ from that of *Cucurbit yellow stunting disorder* crinivirus (CYSDV), and like most other characterized criniviruses, it has a bipartite genome (Kiss et al., 2013). CCYV RNA 1 (8,607 nucleotides), contains four open reading frames (ORFs), the first two of which encode proteins involved in virus replication. CCYV RNA 2 (8,041 nt) contains eight ORFs encoding proteins involved in virus encapsidation and movement (Okuda et al., 2010).

Interestingly, the RNA 1 of most criniviruses downstream of the RNA-dependent RNA polymerase gene (RdRp; Fig. 1) includes 0-3 similarly-sized ORFs encoding proteins that share low levels (25-40%) of amino acid homology. A number of these proteins, including CCYV p22, have been reported to be viral suppressors of RNA silencing (VSRs): *Lettuce chlorosis virus* p23, *Sweet potato chlorotic stunt virus* (SPCSV) RNase3 and p22, *Tomato chlorosis virus* (ToCV) p22, CYSDV p25 and *Tomato infectious chlorosis virus* p27 (Kreuze et al., 2005; Cañizares et al., 2008; Cuellar et al., 2009; Kataya et al., 2009; Kubota & Ng, 2016; Mashiko et al., 2019; Orfanidou et al., 2019; Chen et al., 2019).

These RNA 1-encoded proteins appear to utilize differential modes of action to suppress RNA silencing. For example, SPCSV ORF2 encodes a putative RNase III-like protein (RNase3), which enhances the RNA silencing suppression activity of SPCSV p22 via its endonuclease activity (Kreuze et al., 2005). SPCSV RNase3 binds and subsequently cleaves, long dsRNA molecules and *in vitro* processes siRNAs into ~14 bp products that become inactive in RNA silencing (Cuellar et al., 2008; Weinheimer et al., 2014). For ToCV, the suppression of RNA silencing is mediated by proteins encoded by RNA 1 (p22) and RNA 2 (coat protein, minor coat protein). In common with SPCSV RNase3, ToCV p22 also binds dsRNA, but unlike the former prevents the cleavage of dsRNA molecules by RNase3-type Dicer homologue enzymes (Landeo-Ríos et al., 2016). The RNA-binding ability of the prototype *Lettuce infectious yellows* crinivirus (LIYV) RNA 1–encoded p34 has also been reported (Wang et al., 2010) but its silencing suppressor activity remains in question as studies in the *Nicotiana benthamiana* 16c line did not provide evidence to support its being a VSR (Kiss et al., 2013). Interestingly, LIYV p34 has been shown to be a *trans*-enhancer of RNA 2 replication (Yeh et al., 2000).

Taking into consideration these findings and the reported reduced accumulation of GFP-specific siRNA in GFP/ CCYV p22 co-infiltrated leaf patches (Chen et al., 2019), we examined the ability of CCYV p22 to bind RNA *in vitro*. Our data show that CCYV p22 is able to bind ss, dsRNA and siRNAs and suggests a higher degree of diversity in the modes of action of crinivirus-encoded VSRs.

2. Materials & Methods

2.1 Plasmid construction

The cDNA encoding CCYV p22 was reverse transcribed and PCR amplified from total RNA isolated from of CCYV-infected cucumber plant material (a kind gift of Profs V. Maliogka and N. Katis, University of Thessaloniki), using the specific oligonucleotide primers CCYVp22FBam & CCYVp22RPst (see Table 1). The primers incorporated restriction sites that were subsequently used to introduce the amplicon into a pMAL-c2x expression vector, downstream and in frame with an N-terminal maltose binding protein moiety (MBP-CCYV p22). All recombinant proteins were expressed in BL21/DE3 *Escherichia coli* cells.

2.2 Mutagenesis of CCYV p22

The CCYV p22 deletion mutants were designed to remove four sequential segments of protein, each of them including a cluster of basic amino acids, as these tend to be associated with RNA-binding. The DEL2 deletion lacks amino acid residues 39-75, encompassing the F-box-like motif identified by Chen et al., comprised of residues 53-57. To produce each mutant, the 'round-the-horn' site-directed mutagenesis strategy (Moore, 2015) was employed to delete specific CCYV p22 coding sequences of regions from pMAL c2x-CCYV p22. Briefly, the entire construct minus each desired deletion was PCR amplified as a linear element. The use of Q5 polymerase (NEB) resulted in blunt-ended products without any extraneous nucleotides, and the primers had been 5'-phosphorylated prior to amplification, which facilitated self-ligation of the amplicons with T4 ligase to produce novel MBP fusion constructs ready for expression studies. To create the first deletion (DEL1) lacking amino acids 1-38, the reverse primer CCYVp22Del1R (-1R) corresponded to the plasmid sequence immediately upstream of the CCYVp22 coding sequence, while the forward primer (-1F) was sited immediately downstream of the deletion. The primer pairs used to make the subsequent deletions were designed from the CCYV p22 cDNA sequences flanking each deletion, except for the forward primer (-4F) used to delete of the final segment of the protein which corresponded to the stop codon plus the downstream vector sequence. The double mutant DEL1&2 was made using the primer pair -F2 & -R1. The sequences of all primers are included in Table 1, with a schematic depiction of the fusion proteins shown in Fig 6A.

2.3 Expression in *E. coli* and purification of recombinant proteins

Expression, crude isolation and amylose resin column purification of the MBP protein and the recombinant MBP-ToCV p22, MBP-CCYV p22, MBP-CYSDV p22, MBP-CYSDV p25, and MBP-CCYV p22 deletion mutants was according to the manufacturer's standard protocols (New England Biolabs). Induction of protein expression with 1mM IPTG was all cases carried out at 18 °C for 16 h. The purified proteins were analysed and quantified on 12 % sodium dodecyl sulphate polyacrylamide gel electrophoresis (SDS-PAGE) stained with Coomassie blue dye.

2.4 Preparation of DIG-labelled RNA probes

178
179 Two different DIG-labelled negative sense (-) ssRNA probes were created by transcription of linearized plasmids
180 containing cDNAs corresponding to either a 296 nt fragment derived from *Penicillium stoloniferum* virus F segment 3
181 (PSV-Fs3) or the entire 3' UTR (346 nt) of CCYV RNA 2, that had been linearized with restriction enzymes at the end of
182 the coding sequence, using T3 RNA polymerase in the presence of DIG-11-UTP.
183
184

185
186 A dsRNA probe was created by mixing equimolar amounts of the (-) PSV-Fs3 probe and a homologous (+) sense probe
187 transcribed in the opposite sense from the same plasmid cut at the far end of the cDNA sequence using T7 polymerase.
188 The two strands were allowed to anneal under gradual cooling following heat denaturation.
189
190

191
192 The three small (21, 22 and 24 nt) ssRNAs (5'-GGCAAGUAUAGAGUCAATCCC-3', 5'-
193 GGCAAGUAUAGAAGUCAAUCCC-3', and 5'-GGCAAGUAUAGAUAGUCAATCCC-3'), each incorporating a DIG
194 molecule at its 3' end, have been previously described (Serra-Soriano, 2015).
195
196
197

198 The small DIG-labelled dsRNAs (ds siRNAs) were designed as two complementary 21 nt oligonucleotides (5'-
199 ACUGGAGUUGUCCCAUUCUU-3' and 5'-GAAUUGGGACAACUCCAGUGA-3') with each incorporating a molecule of
200 DIG attached to a 2 nt 3' overhang and synthesized and provided as a duplex (Eurogentec).
201
202
203

204 *2.5 Electrophoretic mobility shift assays*

205
206

207 Nucleic acid-protein interactions were analysed by electrophoretic mobility shift assay (EMSA). For these assays 7 ng of
208 DIG-labelled riboprobe was denatured (5 min at 95 °C), and incubated with either increasing amounts (0-6 µg) of MBP
209 fusion protein, or with 6 µg MBP, for 30 min at room temperature in 1X binding buffer (10 mM Tris-HCl pH 8.0, 100 mM
210 NaCl and 50 % glycerol) with 1U of Recombinant Ribonuclease Inhibitor (NEB). The samples were then resolved in 1 %
211 TAE agarose gels before capillary transfer to positively charged nylon membranes (Hybond-N, GE Healthcare
212 Amersham). Following fixation by baking of the nucleic acids to the membrane (80 °C for 2 h), localization of the DIG-
213 labelled probes was achieved by development with an anti-DIG system (Roche Diagnostics) according to the
214 manufacturer's protocol.
215
216
217
218
219

220 For the EMSAs with the siRNAs, resolution of the products was achieved by different means: the samples incubated with
221 the 21-24 nt ss siRNAs were separated on 5 % polyacrylamide gels (Tris-acetate pH 7.2) at 75 mA for 30 min in 360 mM
222 Tris-pH 7.2, 300 mM NaOAc and 1.1 mM EDTA, with the transfer was achieved using semi-dry electrotransfer in 1X
223 TBE. For the 21 nt ds siRNAs, samples were resolved on 2.5 % TAE agarose gels, and transferred by capillary action.
224
225
226

227 *2.6 Effect of ionic conditions on RNA-binding*

228
229

230 The salt-dependence assay was conducted as above, but using fixed amounts of MBP-CCYV p22 and DIG-labelled
231 PSV-F (-) probe (5 µg, and 7 ng respectively), incubated together with increasing concentrations of NaCl (0, 230, 300,
232 400, 500, 600 and 750 mM) present in the binding buffer.
233
234
235
236

237
238
239
240
241
242
243
244
245
246
247
248
249
250
251
252
253
254
255
256
257
258
259
260
261
262
263
264
265
266
267
268
269
270
271
272
273
274
275
276
277
278
279
280
281
282
283
284
285
286
287
288
289
290
291
292
293
294
295

2.7 Competition assays

For the competition experiments, non-labelled dsRNA of *P. stoloniferum* virus F+S (PSV-F+S) was extracted from virions by phenol-chloroform extraction and ethanol precipitation of a glycerol stock kindly provided by Dr. R. Coutts (University of Hertfordshire, UK). The extract consists of 5 dsRNA elements ranging in size from 677-1753 nt.

3. Results

3.1. CCYV p22 binds single stranded-RNA *in vitro* in a sequence non-specific manner

In order to generate crinivirus RNA1-encoded target proteins CCYV p22, CYSDV p22 and p25 and ToCV p22 (Fig. 1), expression in *E. coli* bacterial cells of the respective MBP-fusions was IPTG-induced overnight at 18°C. This treatment resulted in adequate quantities of intact soluble fusion proteins, which could then be isolated at high purity by amylose column chromatography.

Initially, progressively increasing amounts of each purified MBP-fusion protein was tested in EMSA. In the binding reactions, 7 ng of *in vitro* transcribed DIG-labelled single stranded (ss) RNA was incubated with increasing amounts of purified protein. The electrophoretic mobility of the RNA probe after incubation with the protein was compared with that of the free probe in non-denaturing agarose gels and examined following transfer onto nylon membranes. In these experiments, *Melon necrotic spot virus* (MNSV) coat protein (CP) was used as a positive control for its previously documented ability to bind ssRNA in a non-specific manner (Fig. 1A; Serra-Soriano et al., 2017). When a 390 nt long ssRNA derived from the MNSV 3'-untranslated region (UTR) was used as a probe (Navarro et al., 2006), an alteration on the RNA migration pattern could be observed in the presence relatively large amounts of CCYV p22: an initial RNA shift was detected when 2 µg of protein were used and, when 4 µg or more protein was introduced, a high molecular weight RNA:protein complex could be observed in the upper part of the gel (Fig. 2D). Identical experiments using CYSDV p22 and p25 did not generate any RNA shift (Fig. 2B-C).

The RNA-binding ability of CCYV p22 was further investigated against two more RNA probes. When the complete CCYV RNA 2 3'-UTR (346 nt) was used, a progressive decrease of the free RNA signal could be observed (Fig. 3A). At this point it is important to note that although a heat denaturation step was introduced to relax the secondary structure of the RNA, free RNA population still showed a high proportion of highly structured RNA molecules that disappeared after increasing concentrations of the protein. In an additional EMSA, the 296 nt-long ssRNA probe derived from the *Penicillium stoloniferum* virus F segment 3 (27-322 nt) was used (Fig. 3B). In this assay, a gradual reduction of the free RNA signal could be observed as MBP-CCYV p22 concentrations in the binding reaction progressively increased (1-6 µg), whereas complete disappearance occurred when at least 6 µg of MBP-ToCV p22 was included. Again, the free RNA band disappeared, and the resulting complex, which could not enter the electrophoresis gel, was even difficult to transfer to a nylon membrane (a step required for the detection of the probe; see Materials and Methods section) as

296
297 previously described (Herranz and Pallas, 2004). High concentrations of non-recombinant MBP (expressed and purified
298 under the same conditions as the recombinant MBP-CCYV p22) were also tested. There was no detectable reduction in
299 either free RNA probe or the formation of a retarded RNA:MBP complex, ruling out the possibility that MBP or any
300 contaminating proteins from *E. coli* might contribute to the RNA-binding activity attributed to MBP-CCYV p22.
301 Collectively, these experiments suggested a non-sequence specific ability of CCYV p22 to bind ssRNA *in vitro*.
302
303
304
305

306 3.2. CCYV p22 binds double-stranded RNA molecules

307
308 To check the capability of MBP-CCYV p22 to bind dsRNA molecules, the same quantities of DIG-labeled ssRNA probe
309 and purified MBP-CCYV p22 were incubated in the presence of increasing amounts of unlabeled *Penicillium*
310 *stoloniferum virus* (PSV) genomic dsRNA extracted from purified virions (Buck & Kempson-Jones, 1970; Fig. 4A). In this
311 experiment, the introduction of increasing amounts of a dsRNA competitor (in molar ratios of 1:1, 1:3, 1:10 with the
312 ssRNA probe) resulted in a progressive reversion of the bound ssRNA to a free state (Fig. 4A). To confirm that dsRNA
313 molecules bound to the recombinant MBP-CCYV p22, EMSAs were also carried out using *in vitro* DIG-labelled PSV
314 dsRNA (Fig. 4B). In these experiments, it can be observed that the dsRNA probe was also shifted in a similar manner to
315 that seen with the ssRNA (Fig. 2B) but with lower affinity, as a larger quantity of protein was required to produce the
316 same degree of probe shifting. These results indicate that CCYV p22 binds both ss- and dsRNA in a non-sequence
317 specific manner but in the latter case with apparent lower affinity.
318
319
320
321
322
323
324

325 3.3. The effect of ionic conditions on the *in vitro* binding activity of CCYV p22

326
327 The dependence of CCYV p22 RNA-binding ability on electrostatic interactions was assessed by progressively
328 increasing the NaCl concentration in the incubation mixtures and evaluating the complex dissociation by quantifying the
329 appearance of free RNA *via* film densitometry (Fig. 5). Previous results for MBP-CCYV p22 binding to ss- and dsRNA-
330 (Fig. 3B and 4B), had indicated preferential binding to ss- rather than dsRNA, and similar results were obtained the
331 dependence of this binding on electrostatic interactions was examined. By comparing both IC50s, there appears to be a
332 stronger interaction between CCYV p22 and ssRNA molecules: a 600 mM NaCl concentration was required to reduce
333 the binding to 50 % of the maximal level (Fig. 5B), while only 300 mM NaCl was sufficient to produce the same effect in
334 the case of the dsRNA binding (Fig. 5D). These results reveal a higher stability of the ssRNA-protein complexes, in terms
335 of the NaCl molarity required to dissolve them, that are similar to those observed for some other RNA-binding proteins of
336 viral origin (Brantley & Hunt, 1993; Richmond et al., 1998; Marcos et al., 1999). These observations suggest that the
337 formation of the complex is not solely the consequence of the electrostatic interactions between the RNA and the basic
338 amino acids of p22.
339
340
341
342
343
344
345

346 3.4. Characterization of the RNA-binding domain of CCYV p22

347
348
349 Following characterization of the binding of CCYV p22 to different RNA molecules, attempts were made to identify the
350 particular region of the protein responsible for the RNA binding properties. For this purpose, a set of five MBP-CCYV p22
351
352
353
354

355
356 deletion mutants that together covered the complete length of CCYV p22 were constructed (Fig. 6A). Each MBP-CCYV
357 p22 mutant was utilized in three different amounts (0.3, 3 and 6 μg) in EMSA assays, incubating them with either ss- or
358 dsRNA PSV-derived DIG-labelled probes (Fig. 6B and 6C, respectively). In these experiments, and similarly to full length
359 MBP-CCYV p22, all the mutants were able to bind ssRNA molecules more efficiently (Fig. 6B). Some deletions (del1,
360 del2 and del 1+2) cause the protein to bind with a higher affinity whereas others (del 3 and del 4) bound the probe less
361 efficiently. A similar behaviour was observed for the dsRNA probe (Fig. 6C). These results suggest that the F-box (Chen
362 *et al.*, 2019), which is entirely included in DEL 2, is not essential for ssRNA binding but that within the terminal amino
363 acid residues 76-188 (DEL 3 and DEL 4) there are elements essential for dsRNA binding.
364
365
366
367
368

369 3.5. CCYV p22 exhibits siRNA-binding ability

370
371

372 siRNAs (21, 22 and 24 nucleotides long) are produced when long dsRNA molecules are cleaved by DICERs and
373 constitute key components of the RNA silencing effector complex RISC, providing specificity for downstream targeted
374 degradation of mRNA. Each group interacts with different AGO proteins to produce RISC complexes that confer effective
375 silencing activity (Voinnet, 2005; Pumplin & Voinnet, 2013). The ability of CCYV p22 to bind ss and ds siRNAs was also
376 tested (Fig. 7).
377
378
379
380

381 For this purpose, approximately 7 ng of each of the randomly synthesized ss siRNAs, of 21, 22 or 24 nucleotides (Fig.
382 7A, 7B and 7C, respectively) were incubated with varying concentrations of purified MBP-CCYV p22. As the MBP-CCYV
383 p22 concentration progressively increased, siRNA:protein complexes could be observed to remain in the wells of the gel.
384 It should be noted that the 24 nt-probe required lower amounts of MBP-CCYV p22 to form a detectable complex (Fig.
385 7C).
386
387
388
389

390 The ability of MBP-CCYV p22 to bind to ds siRNAs was also examined. MBP and ToCV p22 were also included as
391 negative controls, as the latter although a strong VSR, has been reported not to bind 21-nt ds siRNAs (Landeo-Ríos *et al.*,
392 2016). As shown in Fig. 7D, identical migration was observed for the 21 nt dsRNA probe whether alone or following
393 incubation with MBP or MBP-ToCV p22. On the contrary, at high concentrations of MBP-CCYV p22 (2-6 μg)
394 ribonucleoprotein complexes with reduced electrophoretic mobility were formed in a concentration-dependent manner.
395
396
397
398

399 4. Discussion

400
401

402 In recent years, it has become apparent that a number of proteins encoded by 3'-proximal ORFs of crinivirus RNA 1 are
403 able to suppress RNA silencing (Kreuze *et al.*, 2005; Cañizares *et al.*, 2008; Cuellar *et al.*, 2009; Kataya *et al.*, 2009;
404 Kubota & Ng, 2016; Mashiko *et al.*, 2019; Orfanidou *et al.*, 2019; Chen *et al.*, 2019) or/and to bind RNA (Wang *et al.*,
405 2010; Weinheimer *et al.*, 2014; Landeo-Ríos *et al.*, 2016). For these proteins, typically expressed from the earliest
406 stages of infection (Klaassen *et al.*, 1996; Salem *et al.*, 2009; Orilio *et al.*, 2014), there is increasing evidence that
407 significant divergence in their manner(s) of action exists.
408
409
410
411
412
413

414
415 Our first EMSA experiments showed that relatively large amounts of MBP-CCYV p22, but not CYSDV p22 and p25, were
416 able to incorporate positive sense ssRNA derived from an unrelated (MNSV 3'-UTR) genomic segment into a complex of
417 high molecular weight. More efficient RNA binding was achieved using the *in vitro*-transcribed 3'-UTR of CCYV RNA2 as
418 the probe, since lower amounts of protein were required to shift it. For all ssRNA probes, the type of RNA:protein
419 complex formed suggested a sequence non-specific type of binding. The gradually decreasing mobility of the probe
420 RNA, observed for both ssRNA or long dsRNAs, is most probably an indication that multiple units of p22 can bind to the
421 RNA, a notion that is supported by the lack of abolishment of the binding by any of the DEL mutants to the ssRNA probe.
422 EMSA results obtained with ss and dsRNA probes revealed a preference of CCYV p22 for ssRNA molecules since a
423 lower amount of protein was required for probe shifting and a higher concentration of NaCl was required to dissociate the
424 RNA:protein complex. These results also suggest that other, non-electrostatic interactions may be involved in the binding
425 process.
426
427
428
429
430
431

432
433 CCYV RNA 1-encoded p22 is a reported weak suppressor of RNA silencing and in coinfiltration experiments in the
434 tissues surrounding the GFP- and p22-infiltrated area, a fine dark zone appeared, indicating there to be no interference
435 with the short-range cell-to-cell movement of RNA silencing signal (Orfanidou et al., 2019). Moreover, CCYV p22 is able
436 to suppress local silencing directly induced by the production of dsRNA, suggesting that it inhibits RNA silencing in
437 parallel with, or downstream of, the production of dsRNA. Northern blots by Chen and co-workers (2019) showed the
438 reduced accumulation of GFP-specific siRNAs in GFP/ p22-agroinfiltrated patches and may indicate a mechanism that
439 alters their abundance or integrity. This observation prompted us to investigate the ability of CCYV p22 to bind RNA.
440 Although a non-specific *in vitro* RNA binding activity alone cannot be used to predict the *in vivo* function of a protein, the
441 finding that CCYV p22 binds *in vitro* ss- and ds siRNAs firstly suggests a connection with its RNA silencing suppression
442 activity, and secondly, that it may contribute to the reduced GFP-specific 24 nt-long siRNAs accumulation reported by
443 Chen et al., (2019). Interestingly, our experiments also show increased binding affinity for the 24 nt-long ss siRNAs.
444
445
446
447
448
449

450
451 CCYV p22 possesses an F-box-like motif essential for the interaction with cucumber SKP1LB1 and for its silencing
452 suppressor activity. However our CCYV p22 DEL2 mutant could still bind ss or dsRNA molecules *in vitro*. For the most
453 intensely-studied crinivirus, LIYV, the binding of RNA by p34 has been proposed to bridge RNA 1-encoded replication
454 proteins to RNA 2, in the only crinivirus identified to date for which the RNA 1 and 2 share no nucleotide conservation at
455 their 3'-UTRs (Kiss et al., 2013). An additional role for CCYV p22 in the virus life cycle cannot be discounted. SPCSV
456 utilizes a VSR (p22) and an RNaseIII-type protein, the latter cleaves siRNAs to effect RNA silencing suppression in a
457 cooperative manner (Weinheimer et al., 2014). The possibility that CCYV p22 may exhibit a similar activity was not
458 addressed in this study. Interestingly, the VSR ToCV p22, which has a stronger and longer lasting effect than CCYV p22,
459 has been shown to preferentially bind long dsRNAs (but not siRNA) and protect them from cleavage (Landeo-Rios et al.,
460 2016). In this context, the present study adds data in the body of information towards a high degree of sophistication in
461 the modes of action and other potential biological role(s) of crinivirus VSRs.
462
463
464
465
466
467

468 **Acknowledgments**

469
470
471
472

473
474
475
476
477
478
479
480
481
482
483
484
485
486
487
488
489
490
491
492
493
494
495
496
497
498
499
500
501
502
503
504
505
506
507
508
509
510
511
512
513
514
515
516
517
518
519
520
521
522
523
524
525
526
527
528
529
530
531

We thank Dr. R. Coutts (University of Hertfordshire, UK) for providing highly purified mycovirus (PSV) virion preparations.

532
533 **Fig. 1.** Schematic representation of the RNA 1 of eight criniviruses. CCYV = *Cucurbit chlorotic yellows virus* (JQ904628);
534 CYSDV = *Cucurbit yellow stunting disorder virus* (NC_004809); BnYDV = *Bean yellow disorder virus* (NC_010560); LCV
535 = *Lettuce chlorosis virus* (NC_012909); SPCSV = *Sweet potato chlorotic stunt virus* (NC_004123); ToCV = *Tomato*
536 *chlorosis virus* (NC_007340); LIYV = *Lettuce infectious yellows virus* (NC_003617), and BYVaV = *Blackberry yellow vein*
537 *associated virus* (NC_006962.2). Different boxes represent specific ORFs: patterned boxes represent ORFs that
538 encoded RNA-binding proteins and grey shaded boxes represent ORFs that code for suppressors of RNA silencing.
539
540
541
542

543 **Fig. 2.** Representative EMSA assays with a DIG-labelled probe from *Melon necrotic spot virus* (MNSV) 3'-untranslated
544 region. MNSV CP was used as a positive control **(A)** and the ssRNA-binding ability of other three crinivirus-encoded
545 proteins was tested: **B)** CYSDV p22, **C)** CYSDV p25 and **D)** CCYV p22. A constant amount of the DIG-labelled RNA
546 probe (7 ng) was incubated with increasing amounts of the proteins (as indicated). To visualize the interactions, after
547 incubation the RNA/protein mixtures were resolved on agarose gels and transferred to nylon membranes. The RNAs
548 were detected with anti-DIG antibody and chemiluminescent substrate.
549
550
551
552

553 **Fig. 3.** Affinity of *Cucurbit chlorotic yellows virus* (CCYV) to different size and nature ssRNA probes. Representative
554 EMSA assays with **A)** 346 nt 3'-UTR RNA 2 CCYV DIG-labelled ssRNA, **B)** 296 nt *Penicillium stoloniferum virus-F* DIG-
555 labelled ssRNA. Maltose binding protein (MBP) and *Tomato chlorosis virus* p22 were used as negative and positive
556 controls, respectively. A constant amount of the DIG-labelled RNA probes was incubated with increasing amounts of
557 MBP-CCYV p22 (as indicated above).
558
559
560
561

562 **Fig. 4.** Representative EMSA assays showing the affinity of *Cucurbit chlorotic yellows virus* (CCYV) p22 to dsRNA
563 molecules in competition analyses where **A)** an unlabeled *Penicillium stoloniferum virus* (PSV) genomic dsRNA
564 extracted from purified virions served as a competitor and **B)** a 296 nt PSV-F DIG-labelled dsRNA probe. Maltose
565 binding protein (MBP) and *Tomato chlorosis virus* p22 were used as negative and positive controls, respectively.
566 Constant amounts (7 ng) of the 346 nt 3'-untranslated region CCYV RNA 2 DIG-labelled ssRNA and MBP-CCYV p22
567 were incubated with increasing amounts of unlabeled PSV dsRNA competitor **(A)** and, a constant amount of the 296 nt
568 PSV-F DIG-labelled dsRNA probe was incubated with increasing amounts of MBP-CCYV p22 **(B)** as indicated above. To
569 visualize the interactions, the RNA/proteins were transferred to nylon membranes and the RNAs detected with anti-DIG
570 antibody and chemiluminescent substrate.
571
572
573
574
575
576

577 **Fig. 5.** Influence of NaCl concentration on the RNA-binding activity of MBP-CCYV p22. Both PSV-F DIG-labelled ss- **(A)**
578 and dsRNA **(C)** probes were incubated alone or with with a constant amount of MBP-CCYV p22 (5 µg) in the presence of
579 increasing concentrations of NaCl, before and the migration of the DIG-labelled RNA probe was analysed by EMSA.
580 Protein-RNA complexes were analysed on a 1 % agarose gel and quantified by densitometry. The fraction of free RNA
581 $[RNA]/[RNA]_t$ was plotted against $[NaCl]$ in mM for the ss- **(B)** and dsRNA **(D)** EMSAs.
582
583
584
585

586 **Fig. 6.** Analysis of RNA-binding properties of *Cucurbit chlorotic yellows virus* (CCYV) p22 deletion mutants. **A)**
587 Schematic representation of the maltose binding protein (MBP)-CCYV p22 fusion protein and its deletion mutants,
588
589
590

591
592 showing the deleted amino acids of each construct on the right. Representative EMSAs showing the affinity of MBP-
593 CCYV p22 fusion protein and its deletion mutants to the 296 nt PSV DIG-labelled ss- **(B)** and dsRNA **(C)** probes. A
594 constant amount of the DIG-labelled RNA probe was incubated with increasing amounts of the fusion proteins for the
595 RNA-binding assay. MBP was used as negative control. To visualize the interactions, the RNA/ proteins were transferred
596 to a nylon membrane and the RNAs detected with anti-DIG antibody and chemiluminescent substrate.
597
598
599
600

601 **Fig. 7.** Affinity of *Cucurbit chlorotic yellows virus* p22 to 21, 22 and 24 nt ssRNAs and 21 nt dsRNAs. Representative
602 EMSAs with **A)** 21, **B)** 22 and **C)** 24 nt DIG-labelled ssRNAs and **D)** 21 bp DIG-labelled dsRNA. A constant amount of
603 the DIG-labelled RNA probe was incubated with increasing amounts of MBP-CCYV p22 (as indicated above each lane).
604 Maltose-binding protein and *Tomato chlorosis virus* p22 were used as negative controls for the 21 nt dsRNA binding
605 assay.
606
607
608
609
610
611
612
613
614
615
616
617
618
619
620

621 References

- 622
623 Abrahamian, P. E., Seblani, R., Sobh, H., & Abou-Jawdah, Y. (2013). Detection and quantitation of two cucurbit
624 criniviruses in mixed infection by real-time RT-PCR. *Journal of Virological Methods*, 193 (2), 320–326.
625
626 Bananej, K., Menzel, W., Kianfar, N., Vahdat, A., & Winter, S. (2013). First Report of *Cucurbit chlorotic yellows virus*
627 infecting cucumber, melon, and squash in Iran. *Plant Disease*, 97 (7), 1005–1005.
628
629 Brantley, J. D., & Hunt, A. G. (1993). The N-terminal protein of the polyprotein encoded by the potyvirus *Tobacco vein*
630 *mottling virus* is an RNA-binding protein. *J Gen Virol*, 74, 1157–1162.
631
632 Buck, K.W. & Kempson-Jones, G.F. (1970). Three types of virus particle in *Penicillium stoloniferum* (1970). *Nature*, 225,
633 945-6.
634
635 Cañizares, M. C., Navas-Castillo, J., & Moriones, E. (2008). Multiple suppressors of RNA silencing encoded by both
636 genomic RNAs of the crinivirus, *Tomato chlorosis virus*. *Virology*, 379 (1), 168–174.
637
638 Chen, S., Sun, X., Shi, Y., Wei, Y., Han, X., Li, H., Chen, L., Sun, B., Sun, H., & Si, Y. (2019). *Cucurbit chlorotic virus*
639 p22
640 protein interacts with cucumber SKP1LB1 and its F-box-like motif is crucial for silencing suppressor activity.
641 *Viruses*, 11 (9), 818.
642
643 Cuellar, W. J., Tairo, F., Kreuze, J. F., & Valkonen, J. P. T. (2008). Analysis of gene content in *Sweet potato chlorotic*
644 *stunt*
645 *virus* RNA1 reveals the presence of the p22 RNA silencing suppressor in only a few isolates: implications for
646
647
648
649

- 650 viral evolution and synergism. *Journal of General Virology*, 89 (2), 573–582.
- 651
- 652 Cuellar, W. J., Kreuze, J. F., Rajamaki, M.-L., Cruzado, K. R., Untiveros, M., & Valkonen, J. P. T. (2009). Elimination of
- 653 antiviral defense by viral RNase III. *Proceedings of the National Academy of Sciences*, 106 (25), 10354–10358.
- 654
- 655 Gyoutoku, Y., Okazaki, S., Furuta, A., Etoh, T., Mizobe, M., Kuno, K., Hayashida, S., & Okuda, M. (2009). Chlorotic
- 656 yellows disease of melon caused by *Cucurbit chlorotic yellows virus*, a new crinivirus. *Japanese Journal of*
- 657 *Phytopathology*, 75, 109–111.
- 658
- 659 Herranz, M.C. & Pallas, V. (2004). RNA-binding properties and mapping of the RNA-binding domain from the movement
- 660 protein of *Prunus necrotic ringspot virus*. *Journal of General Virology* 85, 761-768.
- 661
- 662 Huang, L.-H., Tseng, H.-H., Li, J.-T., & Chen, T.-C. (2010). First report of *Cucurbit chlorotic yellows virus* infecting
- 663 cucurbits in Taiwan. *Plant Disease*, 94 (9), 1168–1168.
- 664
- 665 Kataya, A. R. A., Suliman, M. N. S., Kalantidis, K., & Livieratos, I. C. (2009). *Cucurbit yellow stunting disorder virus* p25
- 666 is
- 667 a suppressor of post-transcriptional gene silencing. *Virus Research*, 145 (1), 48–53.
- 668
- 669 Kiss, Z. A., Medina, V., & Falk, B. W. (2013). Crinivirus replication and host interactions. *Frontiers in Microbiology*, 99 (4),
- 670 1-11.
- 671
- 672 Klaassen, V. A., Mayhew, D., Fisher, D., & Falk, B. W. (1996). *In vitro* transcripts from cloned cDNAs of the *Lettuce*
- 673 *infectious yellows* closterovirus bipartite genomic RNAs are competent for replication in *Nicotiana benthamiana*
- 674 protoplasts. *Virology* 222, 169-175.
- 675
- 676 Kreuze, J. F., Savenkov, E. I., Cuellar, W., Li, X., & Valkonen, J. P. T. (2005). Viral class 1 RNase III involved in
- 677 suppression of RNA silencing. *Journal of Virology*, 79 (11), 7227–7238.
- 678
- 679 Kubota, K., & Ng, J. C. K. (2016). *Lettuce chlorosis virus* p23 suppresses RNA silencing and induces local necrosis with
- 680 increased severity at raised temperatures. *Phytopathology*, 106 (6), 653–662.
- 681
- 682 Landeo-Ríos, Y., Navas-Castillo, J., Moriones, E., & Cañizares, M. C. (2016). The p22 RNA silencing suppressor of the
- 683 crinivirus *Tomato chlorosis virus* preferentially binds long dsRNAs preventing them from cleavage. *Virology*,
- 684 488,
- 685 129–136.
- 686
- 687 Marcos, J. F., Vilar, M., Pérez-Payá, E., & Pallás, V. (1999). *In vivo* detection, RNA-binding properties and
- 688 characterization of the RNA-binding domain of the p7 putative movement protein from *Carnation mottle*
- 689 *carmovirus* (CarMV). *Virology*, 255, 354–365.
- 690
- 691 Mashiko, T., Wang, W. Q., Hartono, S., Suastica, G., Neriya, Y., Nishigawa, H., & Natsuaki, T. (2019). The p27 open
- 692 reading frame of *Tomato infectious chlorosis virus* encodes a suppressor of RNA silencing. *Journal of General*
- 693 *Plant Pathology*, 85, 301–305.
- 694
- 695 Moore, S. (2015). Round-the-horn site-directed mutagenesis. Retrieved from
- 696 https://openwetware.org/wiki/Round-the-horn_site-directed_mutagenesis.
- 697
- 698 Navarro, J.A., Genoves, A, Climent, J., Sauri, A., Martinez-Gil, L., Mingarro, I. & Pallas, V. (2006). RNA-binding
- 699 properties and membrane insertion of Melon necrotic spot virus (MNSV) double gene block movement proteins.
- 700 *Virology* 356: 57-67.
- 701
- 702 Okuda, M., Sugiyama, M., Okuda, S., Okazaki, S., & Yamasaki, S. (2010). Host range and complete genome sequence
- 703
- 704
- 705
- 706
- 707
- 708

- 709
710 of *Cucurbit chlorotic yellows virus*, a new member of the genus *Crinivirus*. *Phytopathology*, 100 (6), 560–566.
- 711 Orfanidou, C., Maliogka, V. I., & Katis, N. I. (2014). First Report of *Cucurbit chlorotic yellows virus* in cucumber, melon
712 and watermelon in Greece. *Plant Disease*, 98 (10), 1446–1446.
- 713 Orfanidou, C., Mathioudakis, M. M., Katsarou, K., Livieratos, I., Katis, N., & Maliogka, V. I. (2019). *Cucurbit chlorotic*
714 *yellows virus* p22 is a suppressor of local RNA silencing. *Archives of Virology*, 164 (11), 2747–2759.
- 715 Orilio, A. F., Fortes, I. M., & Navas-Castillo, J. (2014). Infectious cDNA clones of the crinivirus *Tomato chlorosis virus* are
716 competent for systemic plant infection and whitefly-transmission. *Virology*, 465, 365–374
- 717 Pumplin, N., & Voinnet, O. (2013). RNA silencing suppression by plant pathogens: Defence, counter-defence and
718 counter-counter-defence. *Nature Reviews Microbiology*, 11 (11), 745–760.
- 719 Richmond, K. E., Chenault, K., Sherwood, J. L., & German, T. L. (1998). Characterization of the nucleic acid binding
720 properties of *Tomato spotted wilt virus* nucleocapsid protein. *Virology*, 248, 6–11.
- 721 Salem, N. M., Chen, A. Y., Tzanetakis, I. E., Mongkolsiriwattana, C., & Ng, J. C. (2009). Further complexity of the genus
722 *Crinivirus* revealed by the complete genome sequence of *Lettuce chlorosis virus* (LCV) and the similar temporal
723 accumulation of LCV genomic RNAs 1 and 2. *Virology*, 390, 45–55.
- 724 Serra-Soriano, M. (2015). Relación estructura-función de las proteínas virales implicadas en el movimiento de los
725 carmovirus y su interacción con factores celulares (Doctoral thesis). Retrieved from Riunet
726 (<https://riunet.upv.es>).
- 727 Serra-Soriano, M., Antonio Navarro, J., & Pallás, V. (2017). Dissecting the multifunctional role of the N-terminal domain
728 of the *Melon necrotic spot virus* coat protein in RNA packaging, viral movement and interference with antiviral
729 plant defence. *Molecular Plant Pathology*, 18 (6), 837–849.
- 730 Voinnet, O. (2005). Induction and suppression of RNA silencing: Insights from viral infections. *Nature Reviews Genetics*,
731 6 (3), 206–220.
- 732 Wang, J., Stewart, L. R., Kiss, Z., & Falk, B. W. (2010). *Lettuce infectious yellows virus* (LIYV) RNA 1-encoded P34 is an
733 RNA-binding protein and exhibits perinuclear localization. *Virology*, 403(1), 67–77.
- 734 Weinheimer, I., Boonrod, K., Moser, M., Wassenegger, M., Krczal, G., Butcher, S. J., & Valkonen, J. P. T. (2014).
735 Binding
736 and processing of small dsRNA molecules by the class 1 RNase III protein encoded by *Sweet potato chlorotic*
737 *stunt virus*. *Journal of General Virology*, 95, 486–495.
- 738 Wintermantel, W. M., Jenkins Hladky, L. L., Fashing, P., Ando, K., & McCreight, J. D. (2019). First Report of *Cucurbit*
739 *chlorotic yellows virus* infecting melon in the New World. *Plant Disease*, 778.
- 740 Yeh, H. H., Tian, T., Rubio, L., Crawford, B., & Falk, B. W. (2000). Asynchronous accumulation of *Lettuce infectious*
741 *yellows virus* RNAs 1 and 2 and identification of an RNA 1 trans-enhancer of RNA 2 accumulation. *Journal of*
742 *Virology*, 74 (13), 5762–5768.
- 743
744
745
746
747
748
749
750
751
752
753
754
755
756
757
758
759
760
761
762
763
764
765
766
767

768
769
770
771
772
773
774
775
776
777
778
779
780
781
782
783
784
785
786
787
788
789
790
791
792
793
794
795
796
797
798
799
800
801
802
803
804
805
806
807
808
809
810
811
812
813
814
815
816
817
818
819
820
821
822
823
824
825
826

Table 1 Primer pairs used to create the MBP-CCYV p22 fusion protein and its deletion mutants.

Oligonucleotide Primer			
Name	Primer sequence (5'-3')	Position in CCYV RNA1 Acc. No AB5237788	Use
CCYVp22FBam	GGATCC ATGAATAATCGTAAATTTTCGA	7791 - 7813	cDNA cloning
CCYVp22RPst	CTGCAG TTATATTACGAACTTATTAAGAG	8357 - 8335	cDNA cloning
CCYVp22_Del1F	TTCAGTTTAGATGATGACATAATATACG	7905 – 7932	RTH
CCYVp22_Del1R	GGATCCGAAT CTGAAATCCTTC	7794 - 7895	RTH
CCYVp22_Del2F	GTCACAGAGTATGATGTGTGTG	8016 - 8037	RTH
CCYVp22_Del2R	CAGGAAATATCGACAATCTTTCACA	7904 - 7880	RTH
CCYVp22_Del3F	CTCTCCATTGATGTAGAACTCGA	8184 - 8206	RTH
CCYVp22_Del3R	GAAAAATTCTCTAAACAACCTTGGGT	8105 - 7990	RTH
CCYVp22_Del4F	TAA CTGCAG GCAAGCTTGGCA	8357 - 8354	RTH
CCYVp22_Del4R	AAAAAGTCTTATAAGATCACCGATGG	8183 - 8305	RTH

1. The first line of the document is a header or title, which is mostly illegible due to the low resolution and high contrast of the scan.

2. The second line of the document is a header or title, which is mostly illegible due to the low resolution and high contrast of the scan.

3. The third line of the document is a header or title, which is mostly illegible due to the low resolution and high contrast of the scan.

4. The fourth line of the document is a header or title, which is mostly illegible due to the low resolution and high contrast of the scan.

5. The fifth line of the document is a header or title, which is mostly illegible due to the low resolution and high contrast of the scan.

6. The sixth line of the document is a header or title, which is mostly illegible due to the low resolution and high contrast of the scan.

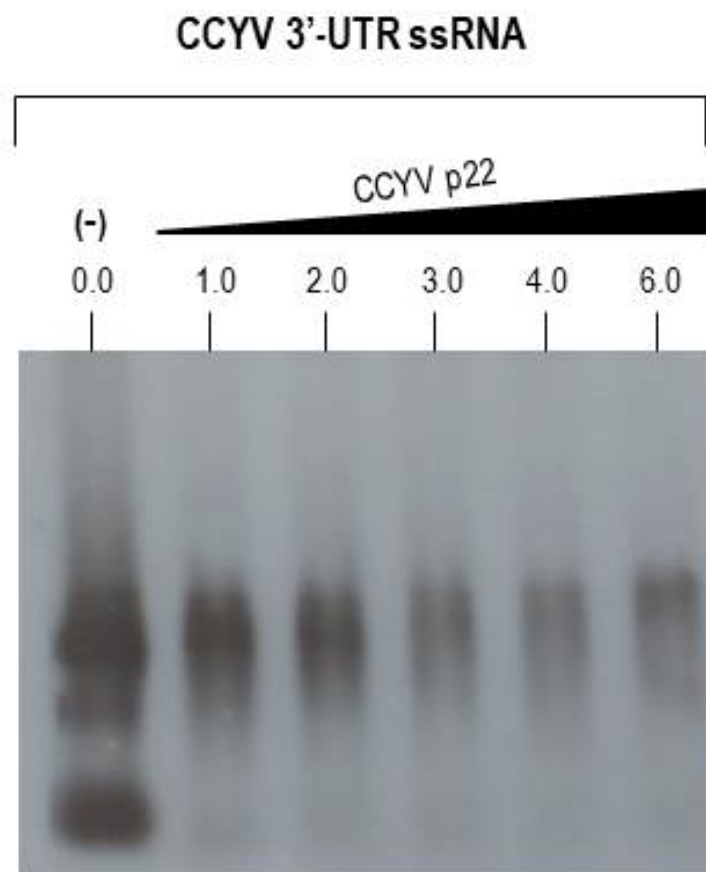
7. The seventh line of the document is a header or title, which is mostly illegible due to the low resolution and high contrast of the scan.

8. The eighth line of the document is a header or title, which is mostly illegible due to the low resolution and high contrast of the scan.

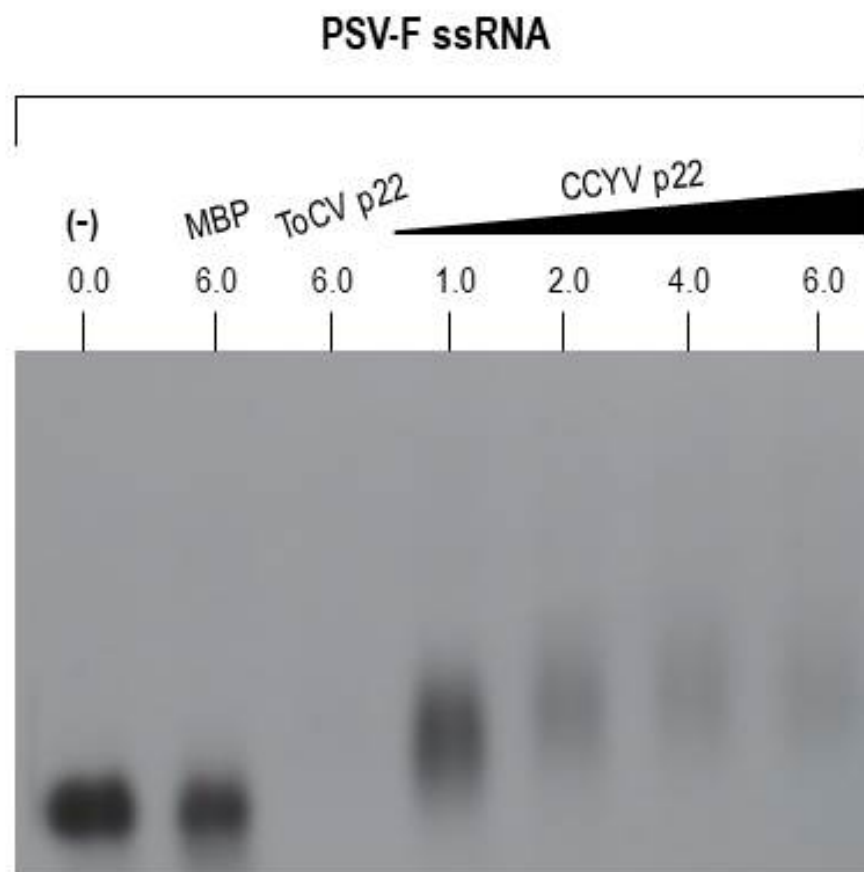
.....

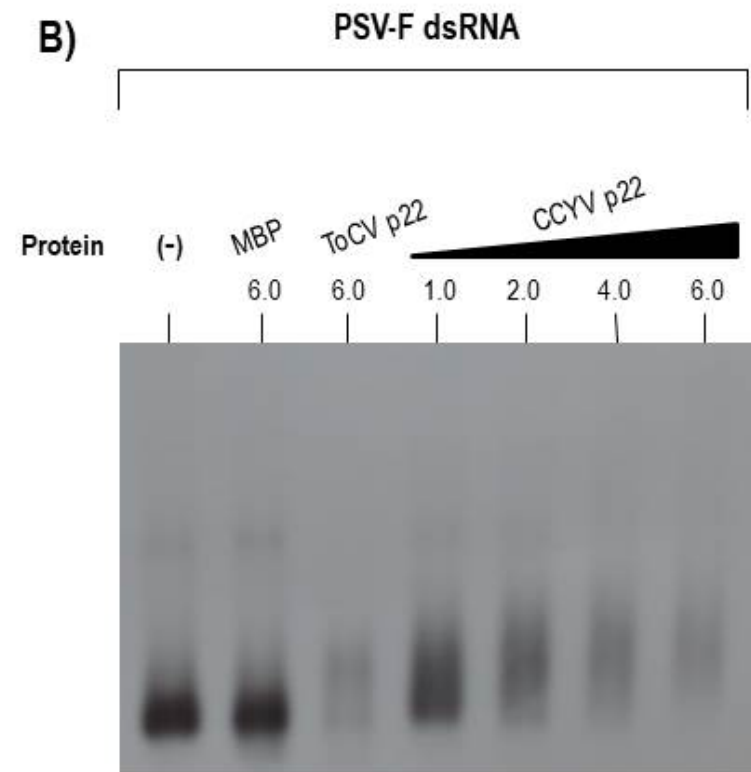
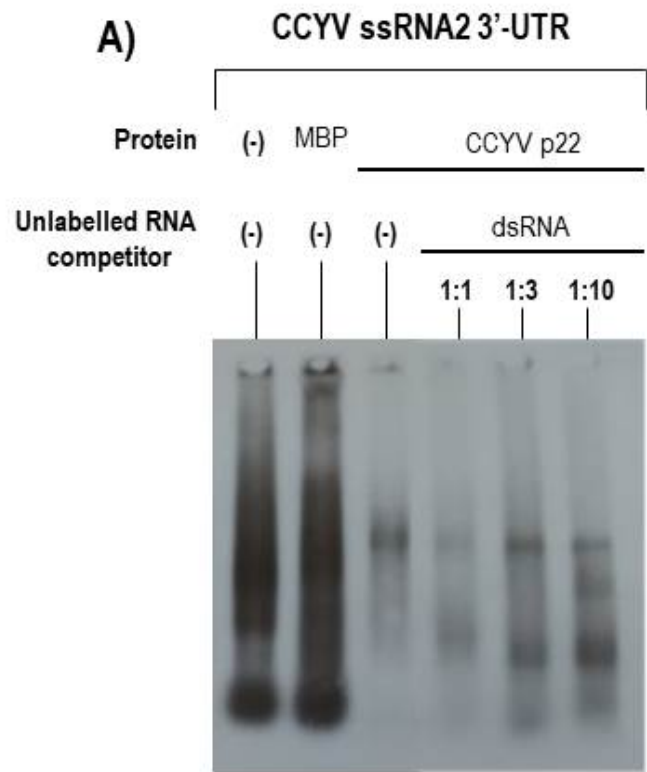
.....

A)

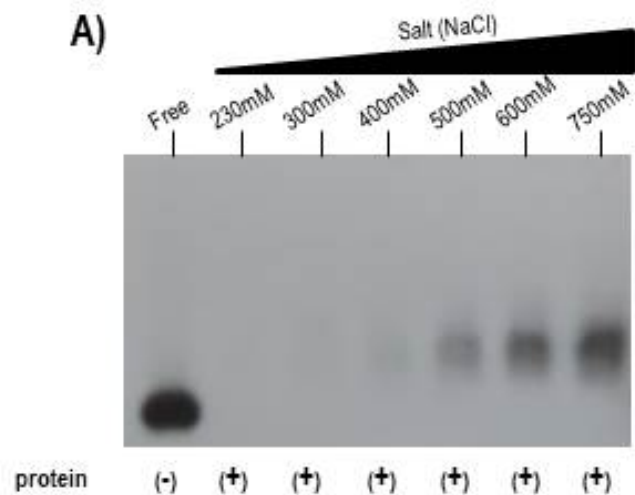


B)

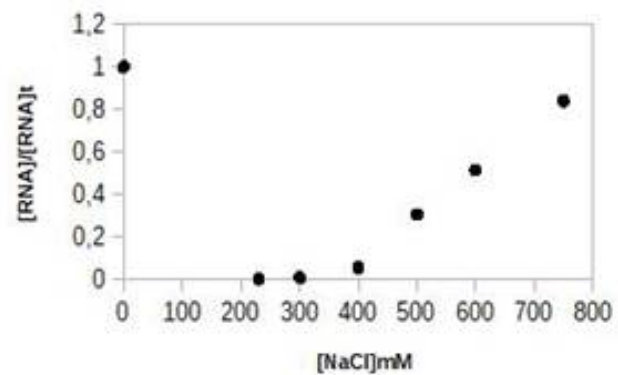




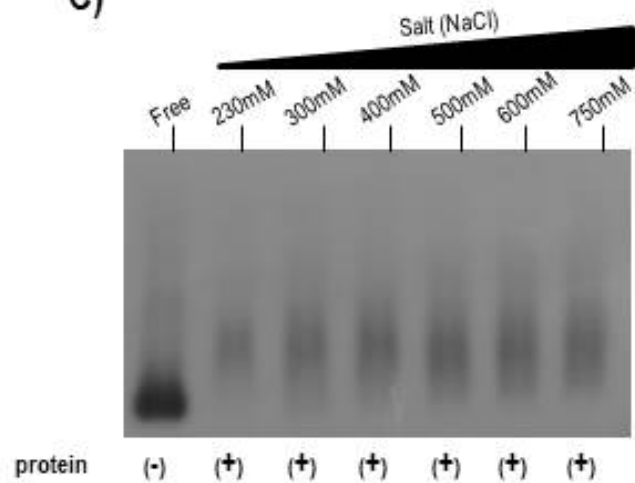
A)



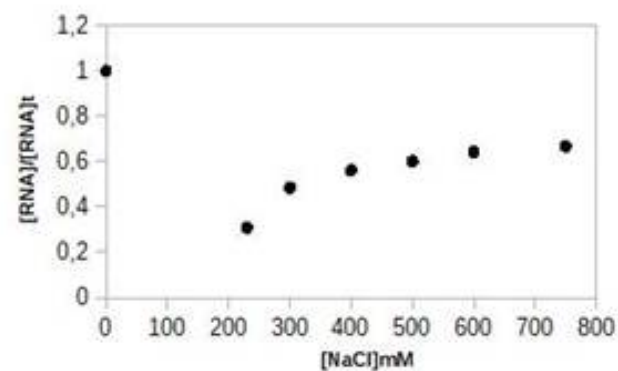
B)

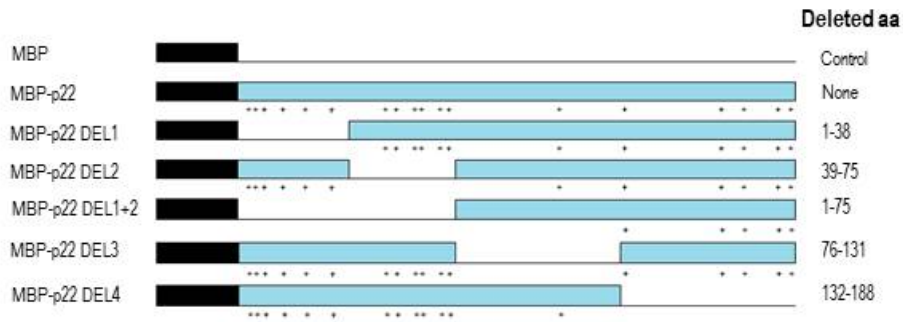
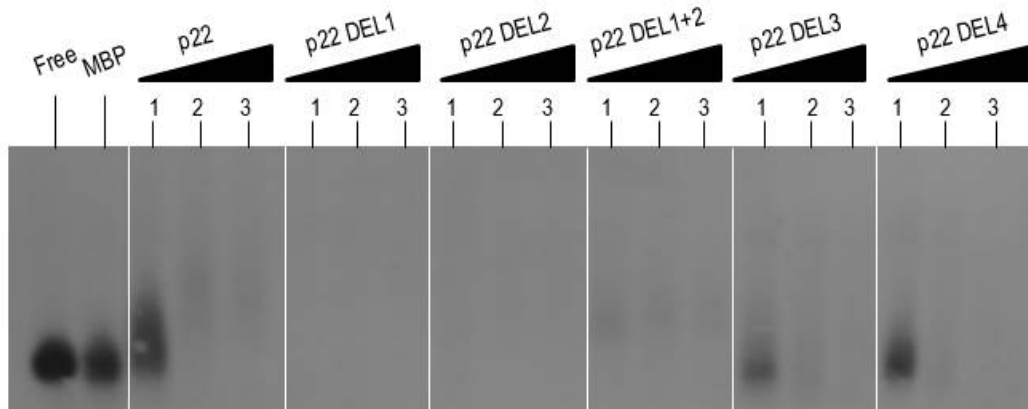
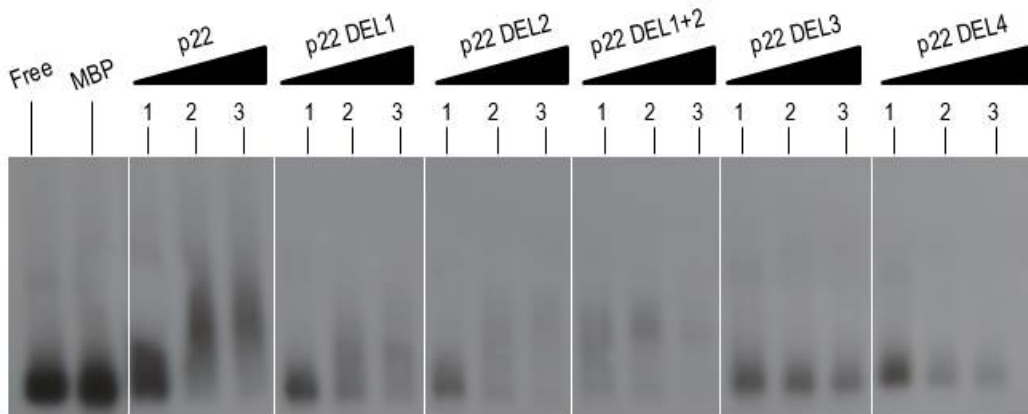


C)



D)



A)**B)****C)**

01201

01201

01201

01201